JACS
JOURNAL OF THE AMERICAN CHEMICAL SOCIETY

Article

pubs.acs.org/JACS

Design and Construction of Higher-Order Structure and Function in Proteinosome-Based Protocells

Xin Huang, Avinash J. Patil, Mei Li, and Stephen Mann*

Centre for Protolife Research and Centre for Organized Matter Chemistry, School of Chemistry, University of Bristol, Bristol BS8 1TS, United Kingdom

Supporting Information

ABSTRACT: The design and construction of higher-order structure and function in proteinosome microcompartments enclosed by a cross-linked membrane of amphiphilic bovine serum albumin/poly(*N*-isopropylacrylamide) (BSA-NH_2/PNIPAAm) nanoconjugates is described. Three structure/function relationships are investigated: (i) differential chemical cross-linking for the control of membrane disassembly and regulated release of encapsulated genetic polymers; (ii) enzyme-mediated hydrogel structuring of the internal microenvironment to increase mechanical robustness and generate a molecularly crowded reaction environment; and (iii) self-production of a membrane-enclosing outer hydrogel wall for generating protease-resistant forms of the protein−polymer protocells. Our results highlight the potential of integrating aspects of supramolecular and polymer chemistry into the design and construction of novel bioinspired microcompartments as a step toward small-scale materials systems based on synthetic cellularity.

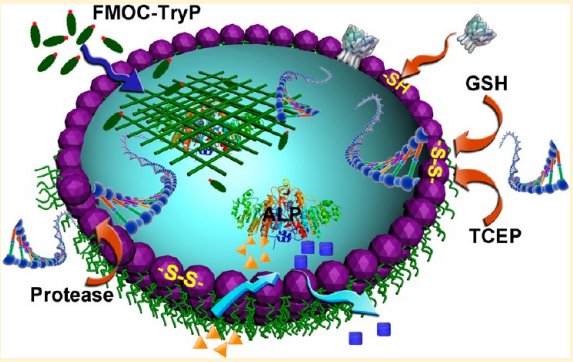

INTRODUCTION

Model cells designed to mimic one or more key aspects of their biological counterparts have been constructed using a range of synthetic microcompartments such as lipid and surfactant vesicles,[1−7] polyelectrolyte capsules,[8−10] polymersomes,[11−14] inorganic colloidosomes,[15−18] aqueous two-phase systems,[19−22] and membrane-free[23−26] or membrane-bounded[27,28] coacervate microdroplets. Integration of various functional components into these enclosed microarchitectures has been exploited to generate synthetic ensembles capable of cell-free gene expression,[1−3,15,21] enzyme-mediated transformations and cascades,[4,8,14,16,17,23,25,28] RNA catalysis,[22] cytoskeletal assembly,[5,6,17] multicompartmentalization,[9,10,12,13,28] membrane growth, reproduction and division,[7,18−20] and motility.[6,11] Taken together, these studies exemplify a modern approach to synthetic cellularity that advances the chemical and physical basis of cell structure and function,[29−32] provides steps toward understanding the emergence of primitive cells on the early Earth,[33,34] and enables the development of future technologies based for example on smart autonomously functioning chemical microcompartments.[29,35,36]

We have recently developed an approach to the construction of a new type of compartmentalized microarchitecture based on the interfacial assembly of globular protein−polymer nanoconjugates at the surface of water droplets dispersed in oil.[37] Approximately three molecules of the temperature-responsive polymer poly(*N*-isopropylacrylamide) (PNIPAAm; M_n = 8800 g mol^{-1}, PDI = 1.19, monomer repeat units ≈ 75) were covalently coupled to the surface primary amine groups of a cationized form of bovine serum albumin (BSA-NH_2), and the resulting amphiphilic BSA-NH_2/PNIPAAm constructs assembled in a water-in-oil emulsion to produce protein-based spherical microcompartments (proteinosomes) typically 20−50 μm and picolitres (1 pL = 10^{-12} L) in diameter and volume, respectively. The proteinosomes consisted of a closely packed monolayer of conjugated globular protein−polymer building blocks with an outer and inner surface of PNIPAAm and protein-rich domains, respectively. Moreover, the membrane could be cross-linked to produce a semipermeable, elastic shell, and as a consequence the intact proteinosomes could be transferred into water with retention of protein function, partially dried and reinflated without loss of membrane structural integrity, and thermally cycled to temperatures of up to 70 °C. Importantly, the transferred proteinosomes could be utilized as a novel type of synthetic protocell that was shown to be capable of selective permeability, guest molecule encapsulation, gene-directed protein synthesis, spatially confined membrane-gated enzyme activity, and membrane-mediated tandem catalysis.[37,38]

Herein, we extend this approach to the preparation of BSA-NH_2/PNIPAAm protocells with new types of higher-order functionality based on controlled membrane disassembly and permeability, internalized assembly of a cytoskeletal-like matrix, and self-production of a membrane-enclosing outer wall. Specifically, we prepare water-filled proteinosomes with

Received: May 1, 2014
Published: June 6, 2014

   dx.doi.org/10.1021/ja504213m | *J. Am. Chem. Soc.* 2014, 136, 9225−9234

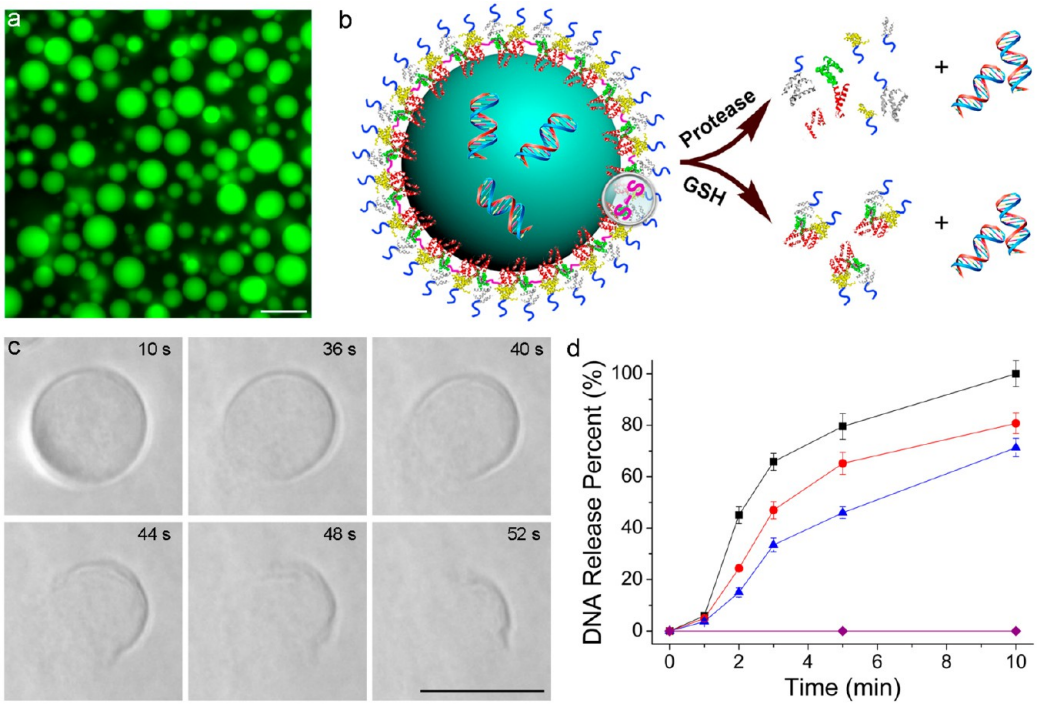

Figure 1. BSA-NH_2/PNIPAAm proteinosomes for DNA encapsulation and release. (a) Fluorescence microscopy image of cross-linked proteinosomes loaded with SYBR green I-stained DNA (2000 bp) after 3 h immersion in a continuous water phase showing no leakage of the entrapped genetic polymer; scale bar, 50 μm. (b) Schematic showing proteinosome membrane disassembly and release of encapsulated DNA by protease-mediated hydrolysis of BSA or GSH-induced cleavage of disulfide cross-links. (c) Time-dependent optical microscopy images showing membrane degradation associated with a NHS-PEG9 ester cross-linked single proteinosome in the presence of protease (1.0 mg/mL). Top row from left to right, 10, 36, 40 s and bottom row, 44, 48, 52 s. Scale bar, 20 μm. (d) Plot showing protease-mediated DNA release from proteinosomes at enzyme concentrations of 50 (black square), 10 (red circles), 2.5 (blue triangles), or 0 (purple diamonds, control) μg/mL.

encapsulated DNA and use protease-mediated hydrolysis of BSA to trigger the rapid disassembly of the microcompartments and concomitant release of the genetic polymer. Alternatively, we exploit two different types of protein cross-links to regulate the release of DNA by chemically induced perforation of the membrane. In addition, we use proteinosome-encapsulated, enzyme-mediated amino acid dephosphorylation as a means of reversibly structuring the internal microenvironment with a supramolecular amino acid hydrogel to increase mechanical robustness and generate a molecularly crowded reaction environment. Finally, we show how prolonged growth of the encapsulated hydrogel results in penetration of amino acid nanofilaments through the porous BSA-NH_2/PNIPAAm shell to produce a continuous outer wall that is positioned adjacent to the external surface of the protein–polymer membrane. As a consequence, the protocells become resistant to protease-mediated degradation. Overall, our results highlight the potential of integrating aspects of supramolecular and polymer chemistry into the design and construction of novel bioinspired microcompartments as a step toward small-scale materials systems based on synthetic cellularity.

RESULTS AND DISCUSSION

Membrane-Mediated Release of DNA from Cross-Linked BSA-NH_2/PNIPAAm Proteinosomes. A dispersion of water-filled proteinosomes with encapsulated SYBR green I-stained DNA ca. 2000 base pairs in length was prepared by the spontaneous assembly of amphiphilic BSA-NH_2/PNIPAAm nanoconjugates at the interface of polynucleotide-containing water droplets in oil (see Experimental Section and Figures S1 and S2).[37] Optical microscopy images showed the presence of structurally stable, nonaggregated hollow microspheres with diameters in the range of 10–25 μm, equivalent to an enclosed confined volume of ca. 1 pL containing approximately 1 million DNA molecules. Cross-linking of the BSA molecules within the proteinosome membrane by reaction of exposed surface amines with bis-*N*-succinimidyl-(nonaethylene glycol) ester (NHS-PEG9 ester; M_W = 709, Figure S3), followed by removal of the oil and dialysis against a series of water/ethanol mixtures, resulted in transfer of the hybrid microcapsules into a continuous water phase without membrane collapse. Significantly, fluorescence microscopy images showed no significant leaching of the genetic polymer into the continuous water phase over several hours (Figure 1a).

Given these observations, we undertook a series of experiments to develop the DNA-loaded proteinosomes as potential microsystems for the storage and release of genetic information (Figure 1b). In particular, we exploited the protease sensitivity of the membrane to induce fast release of the entrapped DNA by enzymatic degradation of the BSA components of the protein–polymer shell. Alternatively, we cross-linked the BSA-NH_2/PNIPAAm membrane with an oligoethylene oxide chain containing a chemically reactive disulfide bridge in place of NHS-PEG9 ester, with the consequence that reductive cleavage of the disulfide bridge by an extraneous reducing agent disassembled the proteinosome microcompartment. Moreover, by using a combination of both nonsulfide and disulfide containing cross-linkers we were able to increase the membrane porosity (via localized S–S cleavage) and trigger DNA release, but without disassembly of the proteinosome shell. Moreover, we show that the highly porous

dx.doi.org/10.1021/ja504213m | J. Am. Chem. Soc. 2014, 136, 9225–9234

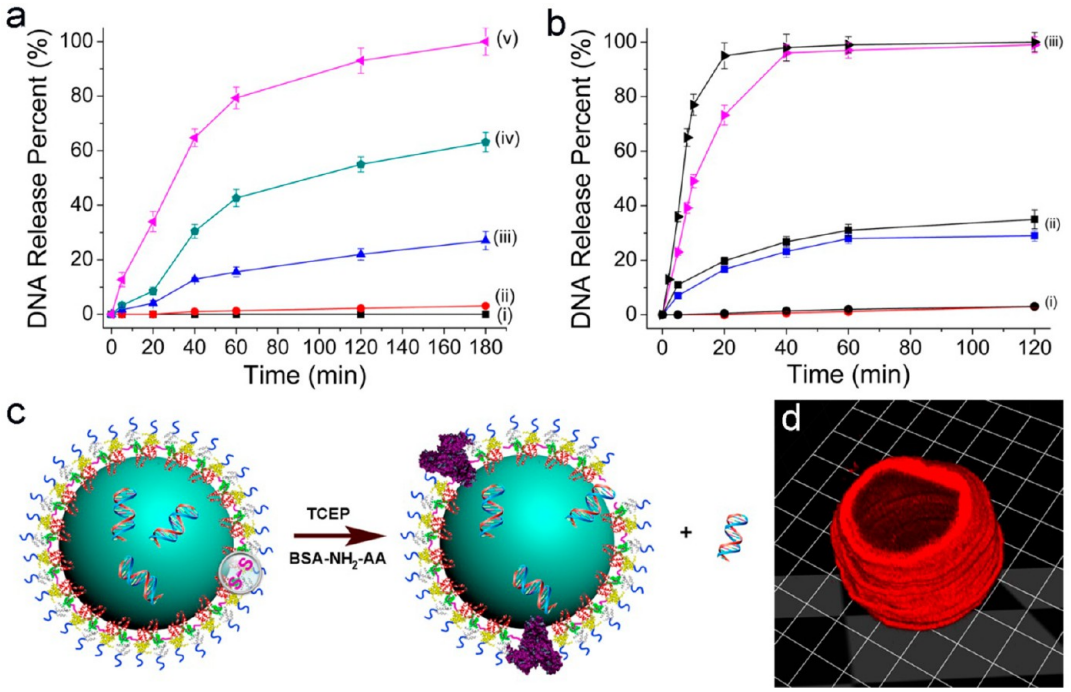

Figure 2. Engineering of proteinosome membrane porosity for regulated DNA release. (a) Plots showing GSH-mediated (5 mM, pH 7.4) release rates of DNA from BSA-NH_2/PNIPAAm proteinosomes cross-linked with both NHS-PEG16-DS disulfide ester and NHS-PEG9 ester bridging groups at respective molar ratios of (i) 0:10, (ii) 1:7, (iii) 4:5.6, (iv) 10:2.8, and (v) 10:0. (b) Plot showing release of DNA from proteinosomes cross-linked with a combination of oligoethylene oxide disulfide and oligoethylene oxide bridging groups associated with a NHS-PEG16-DS: NHS-PEG9 molar ratios of (i) 1:7, (ii) 4:5.6, or (iii) 10:2.8 and incubated with TCEP (5 mM). Corresponding plots in the presence of 5 mg/mL BSA-NH_2-AA (see (c) below) are shown with colored lines. (c) Schematic showing strategy for TCEP-induced partial disassembly and BSA-NH_2-AA resealing of the membrane. (d) 3D confocal image of single proteinosome cross-linked by NHS-PEG16-DS disulfide ester and NHS-PEG9 ester at a molar ratio of 4:5.6 after incubating in 5 mM TCEP and RBITC-BSA-NH_2-AA (5 mg/mL) at pH 8.5 for 2h. The image is consistent with the chemical insertion of BSA-NH_2-AA into the porous membrane.

membranes can be partially resealed using auxiliary BSA molecules comprising surface reactive acrylate groups.

We prepared a water dispersion of DNA-containing BSA-NH_2/PNIPAAm proteinosomes that were cross-linked with NHS-PEG9 ester and added an aqueous solution of protease at concentrations between 0.0025 and 1.0 mg/mL. Optical microscopy video images showed rapid destruction of the proteinosome microarchitecture within 1 min in the presence of 1.0 mg/mL protease (Figure 1c and Movie S1), indicating that enzyme-mediated hydrolysis of the BSA polypeptide chain was facile under these conditions. As a consequence, rapid release of encapsulated SYBR green I-stained DNA over a period of approximately 10 min was observed by fluorescence microscopy as the proteinosome membrane was disassembled (Movie S2). The release profiles were evaluated under different protease concentrations by fluorescence spectroscopy; as anticipated, higher concentrations of protease resulted in more efficient degradation of the proteinosome membrane and correspondingly faster rates of DNA release (Figure 1d).

Alternatively, reduced rates of DNA release from the protein−polymer microcompartments over a period of approximately 2−3 h could be achieved by cross-linking the DNA-containing proteinosomes with PEG-bis(*N*-succinimidyl succinate) disulfide ester (NHS-PEG16-DS ester) instead of NHS-PEG9 ester (Figure S3) and then exposing the colloidal suspension to an aqueous solution of glutathione (GSH, 5 mM; equivalent to intracellular levels of GSH). Release of DNA was accompanied by the slow degradation of the proteinosome membrane associated with reductive cleavage of the inter-conjugate cross-links and solubilization of the BSA-NH_2/PNIPAAm nanoconstructs in the bulk water phase (Figure S4). Significantly, we were able to modulate the release behavior by cross-linking the proteinosomes in the presence of both NHS-PEG16-DS disulfide and NHS-PEG9 esters at various molar ratios. As expected, no release of DNA over several hours was observed for proteinosomes prepared solely with NHS-PEG9 ester cross-links, and increasing the number of disulfide-containing cross-links in the protein−polymer membrane gave rise to an increased rate of membrane rupture and a faster release of the encapsulated DNA (Figure 2a). This was also the case when a stronger reducing reagent (tris(2-carboxyethyl)-phosphine (TCEP)) was used to cleave the disulfide bridges in proteinosomes prepared using mixtures of NHS-PEG16-DS and NHS-PEG9, except that the rates of DNA release were considerably increased such that leakage values close to 100% were achieved after 40 min for microcompartments prepared with NHS-PEG16-DS disulfide ester:NHS-PEG9 ester molar ratios higher than 3.5:1 (Figure 2b). However, in spite of the chemical cleavage of the disulfide-containing cross-links, optical microscopy images indicated that the spherical morphology of the proteinosomes remained intact provided that the membranes were cross-linked with <80% NHS-PEG16-DS (Figure S5). Interestingly, centrifugation of the DNA-depleted proteinosomes followed by reimmersion in an aqueous solution of SYBR green I-stained DNA for 1 h resulted in reloading of the microcompartments with the genetic polymer (Figure S6), while control experiments showed no DNA uptake for water-

dx.doi.org/10.1021/ja504213m | *J. Am. Chem. Soc.* 2014, 136, 9225−9234

filled NHS-PEG16-DS/NHS-PEG9-cross-linked proteinosomes not treated with TCEP or GSH (Figure S7).

Based on these results, we explored whether the ruptured membrane generated by reductive cleavage of proteinosomes prepared with both NHS-PEG16-DS disulfide ester and NHS-PEG9 ester cross-links could be repaired by covalently embedding an auxiliary protein into the porous BSA-NH_2/PNIPAAm shell. For this, we synthesized an acrylic acid-modified cationized BSA (BSA-NH_2-AA) consisting of ca. 17 acrylate groups per molecule (Figure S8 and Experimental Section), with the expectation that a Michael addition reaction involving thiol groups located at the cleavage sites would provide sufficient specificity to reconstitute the partially damaged proteinosome membrane (Figures 2c and S9). To confirm this, we labeled the BSA-NH_2-AA molecules with rhodamine B isothiocyanate (RBITC-BSA-NH_2-AA) and used fluorescence microscopy to monitor the presence of red fluorescence in NHS-PEG16-DS disulfide ester/NHS-PEG9 ester cross-linked proteinosomes incubated in a buffered aqueous solution containing RBITC-BSA-NH_2-AA and TCEP at pH 8.5. Fluorescence microscopy and 3D confocal images showed red fluorescence specifically associated with the protein–polymer microcompartments after 2 h, suggesting that chemical insertion of the auxiliary protein into the porous membrane was successful (Figures 2d and S10). In contrast, no red fluorescence was apparent when RBITC-labeled native BSA was used instead of RBITC-BSA-NH_2-AA. Given these observations, we measured the rate of DNA release from proteinosomes in the presence of both TCEP and BSA-NH_2-AA. The plots indicated that *in situ* resealing of the cleaved cross-links was not sufficient to prevent DNA escape from the microcompartment over a period of 1 h (Figure 2b); however, the rates of release of the genetic polymer were decreased, particularly for capsules cross-linked at relatively high NHS-PEG16-DS:NHS-PEG9 molar ratios.

Enzyme-Mediated Hydrogel Assembly in BSA-NH_2/PNIPAAm Proteinosomes. We used proteinosome-encapsulated, enzyme-mediated amino acid dephosphorylation as a means of reversibly structuring the internal microenvironment of the BSA-NH_2/PNIPAAm protocells. To generate an artificial cytoskeletal-like matrix within the proteinosome interior we added the phosphorylated amino acid derivative, *N*-fluorenylmethyloxycarbonyl-tyrosine-(*O*)-phosphate (Fmoc-TyrP, pH 9.2, sodium carbonate buffer) to the external phase of a room temperature aqueous dispersion of NHS-PEG9 ester-cross-linked BSA-NH_2/PNIPAAm microcompartments containing approximately 80 million alkaline phosphatase (ALP) molecules in an enclosed volume of ca. 1 pL (Figure 3a,b). Uptake of Fmoc-TyrP through the cross-linked proteinosome membrane resulted in enzyme-mediated dephosphorylation of the substrate and concomitant self-assembly of a *N*-fluorenylmethyloxycarbonyl-tyrosine (Fmoc-TyrOH) nanofilament-based hydrogel specifically within the microcompartment interior (Figures 3c and S11). This was confirmed by optical and fluorescence microscopy images recorded on individual proteinosomes 7 h after addition of Fmoc-TyrP to the aqueous continuous phase. Co-location of the BSA-NH_2/PNIPAAm membrane, encapsulated ALP, and entrapped Fmoc-TyrOH hydrogel was confirmed by preparing proteinosomes from fluorescently labeled proteins and encapsulating the nanofilament-binding fluorescent dye, Hoechst 33258 (blue fluorescence on binding) within the microcompartment interior (Figure 3d–g). 3D confocal fluorescence images confirmed that

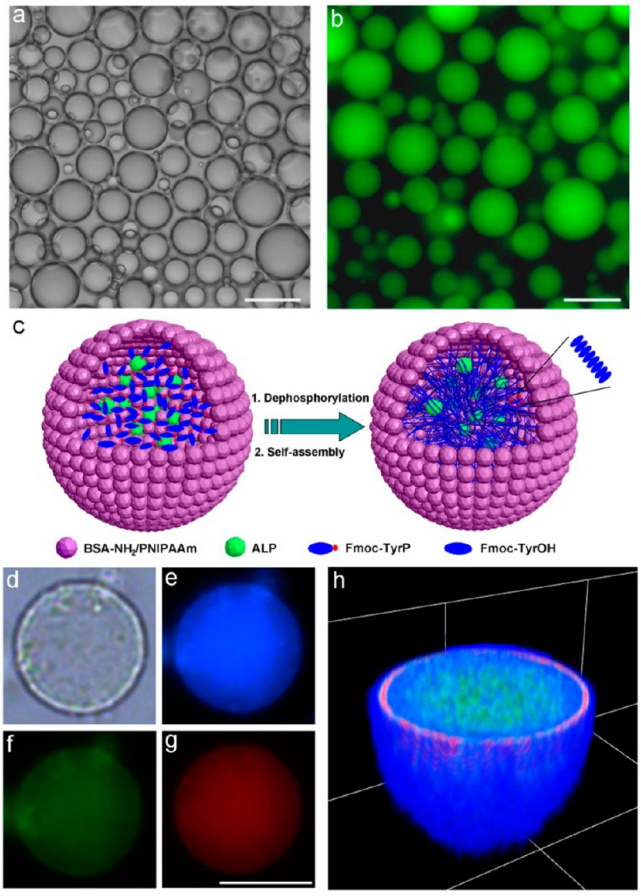

Figure 3. Enzyme-mediated self-assembly of a cytoskeletal-like hydrogel network within ALP-containing BSA-NH_2/PNIPAAm proteinosomes. (a) Optical microscopy image of ALP-containing proteinosomes dispersed in oil and (b) fluorescence microscopy image after NHS-PEG9 ester cross-linking and transfer into water; scale bars, 20 μm. The green fluorescence in (b) is associated specifically with the proteinosome interior and originates from FITC-labeled ALP confined within the microcompartments. (c) Schematic representation showing formation of a Fmoc-TyrOH nanofilament hydrogel network inside a proteinosome microcompartment by ALP-mediated dephosphorylation of Fmoc-TyrP. The amino acid substrate is added to the external continuous water phase while the enzyme is incarcerated in the proteinosome interior. (d) Optical and (e–g) fluorescence microscopy images of a single hydrogel proteinosome; (e) blue fluorescence image associated with binding of encapsulated Hoechst 33258 dye to Fmoc-TyrOH nanofilaments, (f) green fluorescence corresponding to FITC-BSA-NH_2/PNIPAAm nanoconjugates in the proteinosome membrane, and (g) red fluorescence corresponding to rhodamine B isothiocyanate-tagged-ALP (RBITC-ALP) encapsulated inside the proteinosome; scale bar, 10 μm. (h) Confocal fluorescence microscopy image of a hydrogel-containing single proteinosome (reaction time, 7 h) showing spatially segregated areas of red, blue, and green fluorescence corresponding to the protein–polymer membrane (RBITC-BSA-NH_2/PNIPAAm), Fmoc-TyrOH hydrogel (Hoechst 33258) and encapsulated ALP (FITC-ALP) immobilized within the entrapped hydrogel matrix.

ALP-mediated assembly of the Fmoc-TyrOH hydrogel often resulted in complete filling of the microcompartment after 7 h to produce a structured interior containing immobilized enzyme molecules (Figure 3h).

We monitored formation of the amino acid hydrogel within single proteinosomes by measuring time-dependent increases in Hoechst 33258 blue fluorescence intensity over a period of

dx.doi.org/10.1021/ja504213m | *J. Am. Chem. Soc.* 2014, 136, 9225–9234

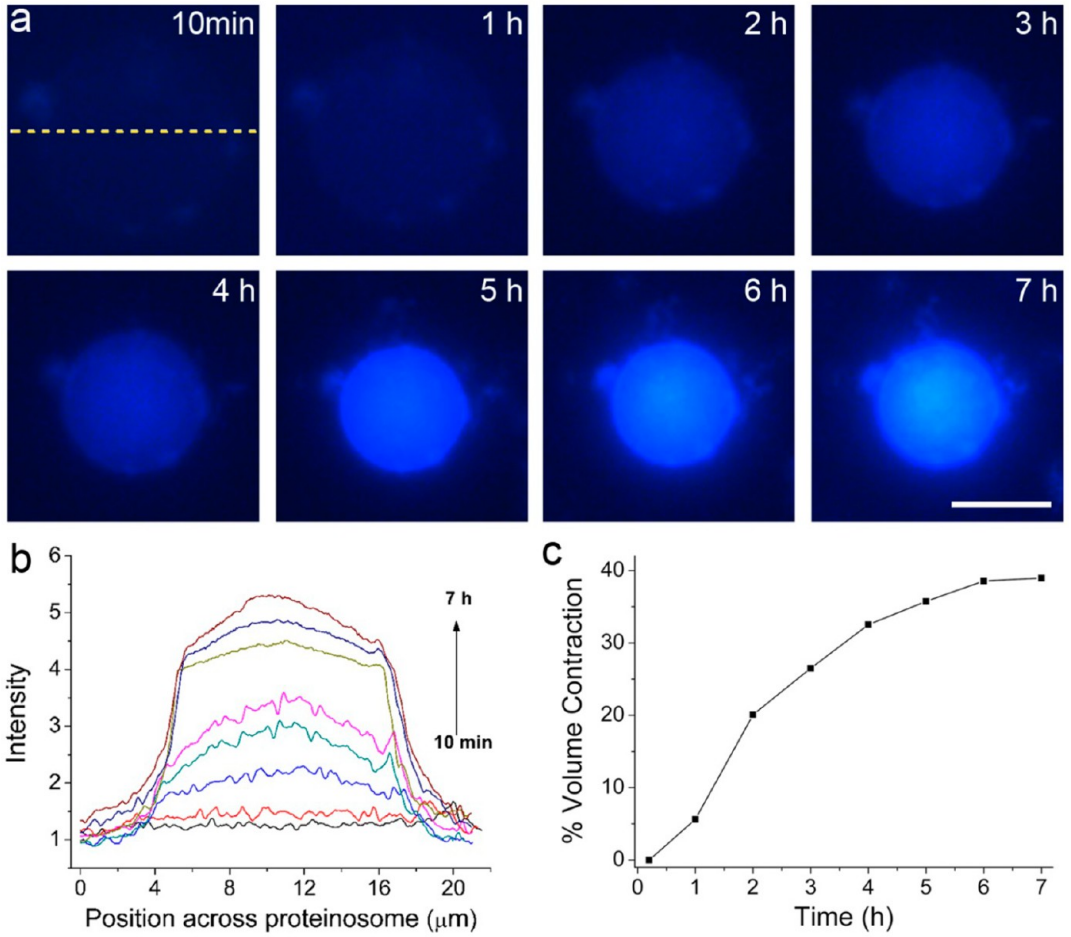

Figure 4. Fmoc-TyrOH hydrogel growth in ALP-containing BSA-NH_2/PNIPAAm proteinosomes. (a) Time-dependent fluorescence microscopy images showing *in situ* formation of a FMOC-TyrOH hydrogel within a single proteinosome as monitored by the fluorescence emission intensity associated with Hoechst 33258 binding to the amino acid nanofilament; scale bar, 10 μm. (b) Fluorescence line intensity profiles recorded across the single proteinosome shown in (a) (yellow line) at various times after addition of Fmoc-TyrP. (c) Plot showing time-dependent contraction in proteinosome volume associated with hydrogel formation within the microcompartment.

several hours (Figure 4a,b). The data indicated that primary nucleation of the nanofilaments within the picolitre volume occurred within 1 h of adding Fmoc-TyrP to the external water phase and was followed by a period of relatively linear growth over 5 h (Figure S12). Interestingly, corresponding measurements of the diameter of single BSA-NH_2/PNIPAAm proteinosomes during internalized growth of the supramolecular hydrogel showed a 40% decrease in size over 7 h (Figures 4c and S13). Control experiments showed no significant volume (density) change of the hydrogel when prepared in bulk aqueous solution, and mixing water-filled (enzyme-free) proteinosomes with FMOC-TyrP solution for up to 7 h gave only a 2.5% change in the volume. We therefore attributed the large volume contraction observed for the ALP-containing proteinosomes to hypertonic conditions arising from a sustained Fmoc-TyrP concentration gradient across the membrane due to continual consumption of both the substrate (via enzyme-mediated dephosphorylation) and Fmoc-TyrOH product (via assembly into nanofilaments) inside the proteinosome.

We investigated whether formation of the supramolecular hydrogel within the proteinosomes could give rise to functional microcompartments capable of morphological deformation and self-healing behavior when exposed to mechanical stresses at room temperature in an aqueous environment. For example, when mechanically deformed by a soft plastic fiber, the spherical morphology of the hydrogel-containing proteinosomes was re-established within 60 s (Figure 5a and Movie S3). In contrast, BSA-NH_2/PNIPAAm proteinosomes prepared without internal structuration collapsed irreversibly under the same conditions (Figure S14), indicating that supramolecular gelation within the microcompartments considerably increased the robustness of the microarchitecture. Moreover, the hydrogel-containing proteinosomes could withstand complete dehydration, such that the deflated microcapsules produced on drying could be reinflated to the native spherical morphology by adding water (Figure 5b,c and Movie S4). In contrast, the water-filled proteinosomes collapsed irreversibly on dehydration.

Other experiments indicated that the self-assembled Fmoc-TyrOH nanofilaments could be partially disassembled within the proteinosome interior by increasing the temperature to the gel−sol transition temperature (ca. 45 °C). This was evidenced by the corresponding decrease in the fluorescence intensity associated with nanofilament disintegration and concomitant release of the bound Hoechst 33258 dye molecules (Figure 5d,e). The results indicated that the internal viscosity of the BSA-NH_2/PNIPAAm proteinosomes could be modulated by

dx.doi.org/10.1021/ja504213m | J. Am. Chem. Soc. 2014, 136, 9225−9234

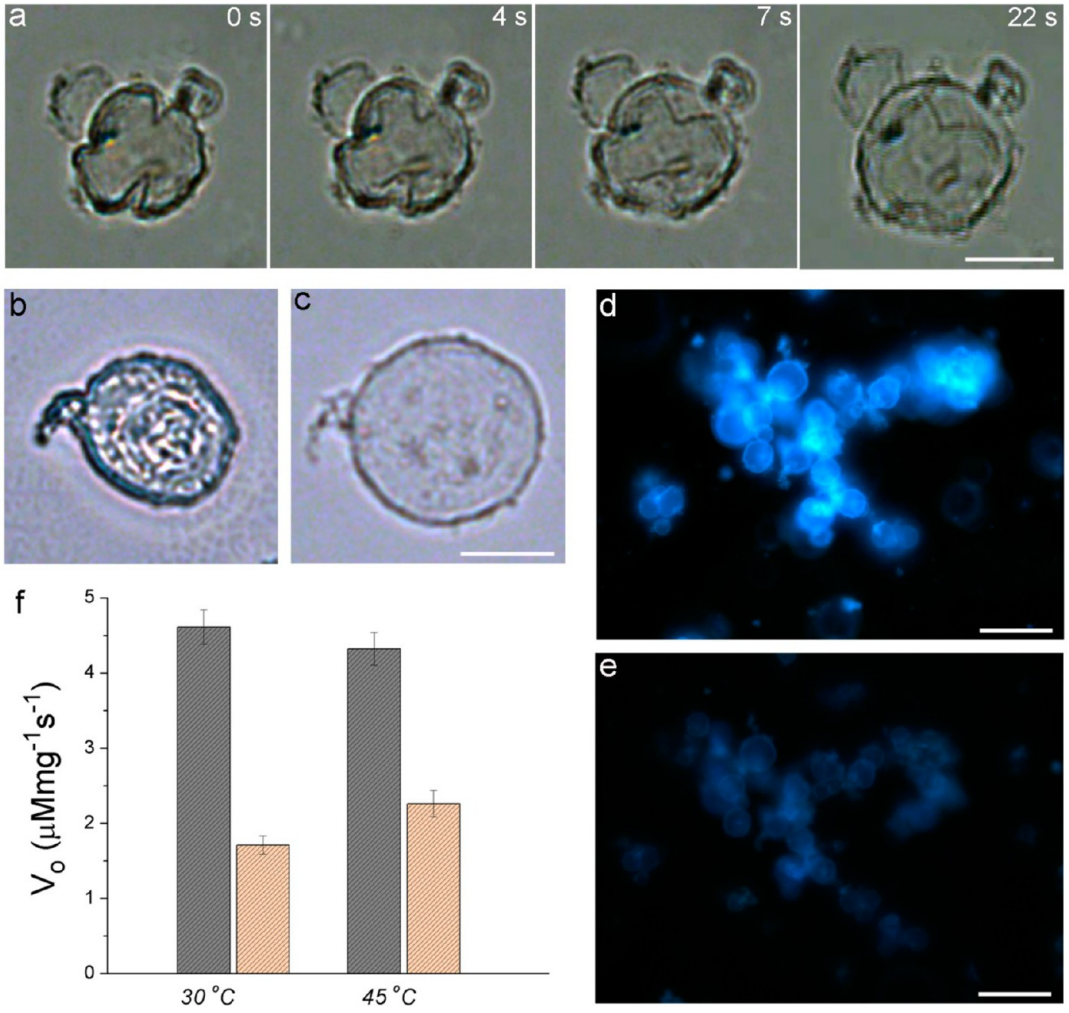

Figure 5. Mechanical and chemical properties of hydrogel-containing BSA-NH_2/PNIPAAm proteinosomes. (a) Time-dependent optical microscopy images showing self-healing behavior of a single hydrogel proteinosome subjected to deformation using a soft plastic fiber; scale bar, 10 μm. (b,c) Optical microscopy images of a single hydrogel proteinosome after drying in air (b) and rehydration (c); scale bars, 10 μm. (d,e) Fluorescence microscopy images of a hydrogel-containing proteinosome containing Hoechst 33258 at 25 °C (d) and at the gel−sol transition temperature (45 °C) after 10 min (e). (f) Initial rates of ALP-mediated dephosphorylation of *p*-nitrophenyl phosphate (5 mM, pH 8.8) before (gray columns) and after (orange columns) hydrogel formation at 30 or 45 °C (below and at the gel−sol transition temperature, respectively).

controlling the noncovalent interactions between the Fmoc-TyrOH molecular building blocks and suggested that such changes might be used to influence the enzymatic activity of the encapsulated ALP molecules depending on whether the enzyme was embedded in the entrapped hydrogel or dispersed in an aqueous solution of Fmoc-TyrOH monomers. We tested this possibility by adding the small molecule substrate, *p*-nitrophenyl phosphate (PNPP, 5 mM), to the continuous water phase of a suspension of water-filled or hydrogel-containing ALP-encapsulated BSA-NH_2/PNIPAAm proteinosomes at 30 °C and measuring the corresponding initial rates of formation of *p*-nitrophenolate at pH 8.8 by UV−vis spectroscopy. Similar experiments were undertaken for the water-filled or hydrogel-containing ALP-encapsulated proteinosomes at 45 °C (Figure 5f). At 30 °C, the water-filled enzymatically active proteinosomes were almost three times more active than the ALP-encapsulated hydrogel proteinosomes, presumably due to kinetic constraints associated with slow diffusion of the substrate through the viscous supramolecular gel. In contrast, while the initial rate associated with the water-filled proteinosomes was reduced by 6.3% at 45 °C, partial disassembly of the entrapped Fmoc-TyrOH network to produce a solution of amino acid monomers at this temperature gave rise to a 32% increase in the initial rate. The results were consistent with a decrease in the viscosity of the local environment within the BSA-NH_2/PNIPAAm proteinosomes at the gel−sol transition temperature. However, the rate of enzyme activity within the proteinosomes at the critical temperature was not restored to the values obtained for the continuous aqueous phase, suggesting that disassembly of the hydrogel was not complete or that PNPP dephosphorylation was inhibited inside proteinosomes containing high concentrations of Fmoc-TyrOH oligomers or both.

Outer Wall Self-Assembly in Hydrogel-Containing BSA-NH_2/PNIPAAm Proteinosomes. Formation of a hydrogel microsphere inside the BSA-NH_2/PNIPAAm proteinosomes was completed typically after 7 h. However, the continued presence of a large excess of Fmoc-TyrP in the external phase as well as active ALP molecules embedded within the hydrogel suggested that dephosphorylation of the amino acid was still possible after this time period provided that diffusion of the reactant into the hydrogel interior was still

dx.doi.org/10.1021/ja504213m | *J. Am. Chem. Soc.* 2014, 136, 9225−9234

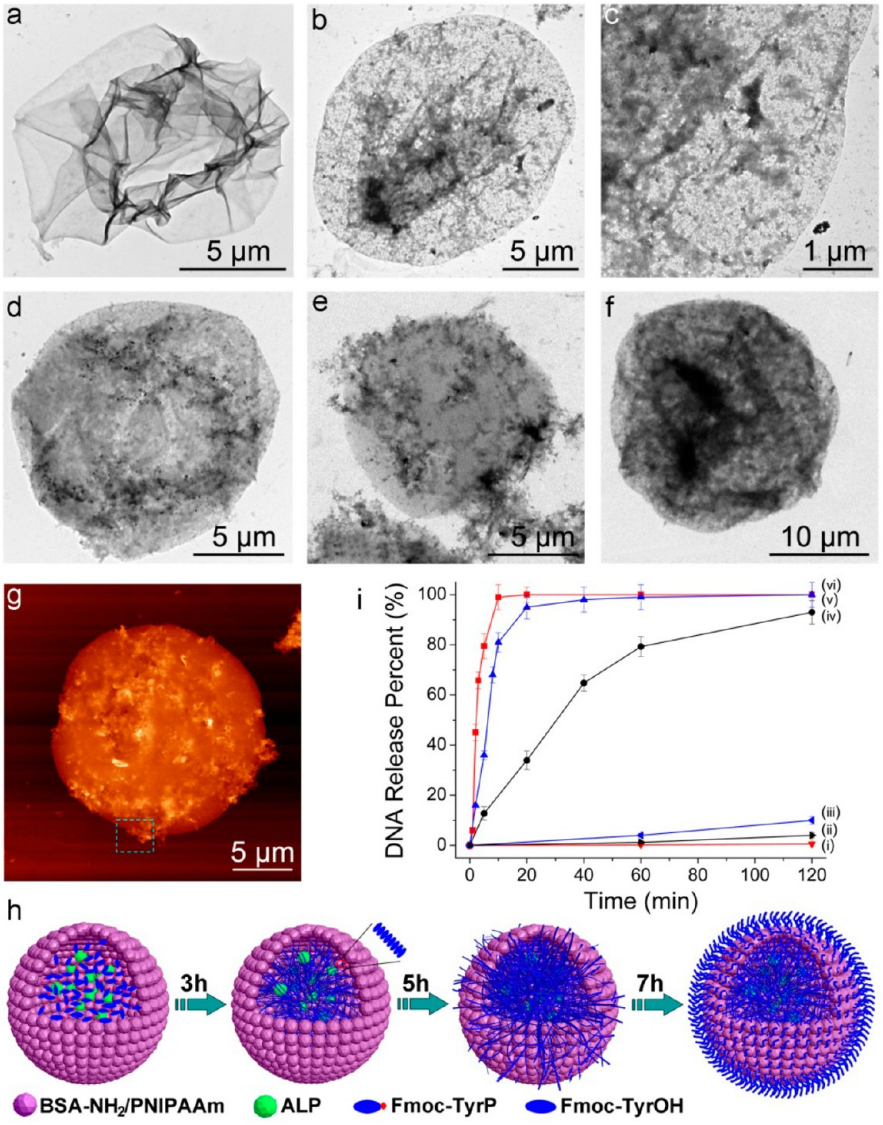

Figure 6. Outer wall formation and DNA release by hydrogel-modified BSA-NH_2/PNIPAAm proteinosomes. (a–f) TEM micrographs of water-filled proteinosomes (a) and hydrogel-containing proteinosomes after 1 (b,c), 3 (d), 5 (e) and 7 h (f). Note the increase in hydrogel density with time, the smooth membrane surface in (a–c) and outer wall formation in (d–f). (g) AFM image showing roughened texture on the outer surface of a single hydrogel-modified proteinosome after 7 h. High-magnification image and height profile of boxed area are shown in Figure S15. (h) Scheme showing time-dependent development of a membrane-enclosing outer wall in hydrogel-modified proteinosomes. (i) Plot showing negligible DNA release from NHS-PEG16-DS cross-linked hydrogel-modified proteinosomes in the presence of (i) protease (50 μg/mL), (ii) GSH (5.0 mM), or (iii) TCEP (5.0 mM) due to outer wall formation and membrane protection. (iv–vi) Corresponding plots for water-filled proteinosomes showing rapid membrane disassembly and DNA release in the presence of (iv) GSH (5.0 mM), (v) TCEP (5.0 mM), or (vi) protease (50 μg/mL).

possible. Indeed, localized outgrowths that extended outside the boundary of the protein–polymer microcompartments were often observed after approximately 5 h in the fluorescence microcopy images (see Figure 4a for example), suggesting that the Fmoc-TyrOH reaction product diffused through the semipermeable membrane into the continuous water phase as the interior became densified with the supramolecular hydrogel. This was confirmed by TEM investigations of proteinosomes at various stages of hydrogel formation. TEM images of single water-filled proteinosomes showed the presence of a highly electron transparent, intact membrane that collapsed in the vacuum of the electron microscope (Figure 6a). In contrast, ALP-containing proteinosomes imaged within 1 h of adding Fmoc-TyrP showed partially collapsed microcapsules in association with a low-density matrix of electron dense material that was attributed to the early stages of formation of the Fmoc-TyrOH hydrogel (Figure 6b). Moreover, the proteinosomes exhibited a smooth surface texture (Figure 6c), suggesting that the hydrogel was specifically located within the interior of the microcompartments. The density of the hydrogel phase was increased considerably after 3 h to produce proteinosomes that were imaged as noncollapsed, electron dense microspheres with a regular morphology and homogeneous core (Figure 6d). Significantly, the latter were partially covered with extraneous electron dense material that appeared to be loosely attached after 5 h (Figure 6e) but firmly associated with the outside of the proteinosome membrane after 7 h (Figure 6f). AFM images indicated that the surface texture consisted of a network of entangled nanofilaments, often 2–4 nm in thickness (Figures 6g and S15). We attributed these observations to the

dx.doi.org/10.1021/ja504213m | J. Am. Chem. Soc. 2014, 136, 9225–9234

spontaneous formation of a thin hydrogel shell on the external surface of the protein−polymer membrane via secretion of Fmoc-TyrOH from the internally driven enzyme reaction (Figure 6h). Leaving the reaction for 24 h increased the thickness of the proteinosome outer wall without disruption of the inner membrane such that the microcompartments became aggregated and immobilized within an extra-protocellular hydrogel matrix (Figure S16).

We tested whether the self-production of a membrane-enclosing outer wall by the BSA-NH_2/PNIPAAm proteinosomes could elicit resistance to enzyme-mediated or chemically induced disassembly of the protein−polymer inner shell. For this, we prepared NHS-PEG16-DS disulfide ester cross-linked proteinosomes containing both ALP and DNA, transferred the dispersion into water, incubated the samples in Fmoc-TyrP for 7 h to generate an internal hydrogel matrix and external hydrogel wall, and then monitored the release of DNA in the presence of a protease, TCEP or GSH. Significantly, while a protease concentration of 50 μg/mL disassembled the proteinosome membrane within 10 min for the water-filled microcompartments (see Figure 1d), essentially no release of DNA was observed within 1 h for the protease-treated proteinosomes after hydrogelation (Figures 6i and S17), indicating that the protein−polymer membrane was resistant to hydrolytic degradation under these conditions. Control experiments using DNA-containing membrane-free hydrogel fragments showed rapid release of the polynucleotide within 7 min of immersion in water (Figure S18). Experiments undertaken in the presence of 5 mM external concentrations of TCEP or GSH also showed highly reduced rates of DNA release compared with the water-filled proteinosomes (Figure 6i). In the presence of TCEP, virtually no release was observed from the hydrogel-modified proteinosomes within the first 20 min compared with a leakage value of 90% in the water-filled microcompartments over this time period. Similarly, DNA release values of 90 or 5% where measured for the water-filled or hydrogel-modified proteinosomes, respectively, when incubated in aqueous solutions of GSH for 120 min. Leaving the hydrogel-modified proteinosomes for 30 h in the presence of the protease, GSH or TCEP gave release values of 20, 70, and 100% (Figure S19), indicating that the outer wall remained essentially impermeable to the protein macromolecules over this time period. In contrast, the small-molecule reducing agents were able to diffuse through the outer wall and react with the disulfide ester membrane cross-links to produce modified microcompartments exhibiting slow release behavior.

CONCLUSIONS

In this paper, we describe the preparation of BSA-NH_2/PNIPAAm proteinosomes with three new types of higher-order functionality. First, we use enzyme-mediated disassembly or differential chemical cross-linking to modulate membrane porosity and trigger the slow or fast release of polynucleotides encapsulated within the protein−polymer microcompartments. We also show that the highly porous membranes can be partially resealed using auxiliary BSA molecules comprising surface reactive acrylate groups. Second, we use proteinosome-encapsulated, enzyme-mediated amino acid dephosphorylation as a means of reversibly structuring the internal microenvironment with a supramolecular amino acid hydrogel to increase mechanical robustness and generate a molecularly crowded reaction environment. Finally, we show that prolonged growth of the encapsulated hydrogel results in the formation of a continuous outer wall that surrounds the proteinosome membrane and provides chemical resistance to protease-mediated disassembly.

Taken together, our results highlight the potential of integrating aspects of supramolecular and polymer chemistry into the design and construction of proteinosome-based microcompartments. There are relatively few other examples of microcompartments based on amphiphilic protein self-assembly.[39] The ability to manipulate the structure and function of microscale ensembles based on proteinosomes should provide novel opportunities in cytomimetic engineering, bioinspired microstorage and delivery, microreactor technologies, and bottom-up synthetic biology. Moreover, the self-production of a proteinosome membrane-enclosing outer wall by an internally generated reaction could have important implications as it provides a first step toward a protocell model that incorporates cell wall formation as an integral aspect of membrane-bounded compartmentalization. In this regard, we note that multilayered cell surface architectures are ubiquitous in simple organisms such as bacteria and Archaea, and mimicking cell wall/plasma membrane formation could therefore offer insights into how these integrated structures might have been assembled within a prebiotic context.

EXPERIMENTAL SECTION

Synthesis of BSA-NH_2/PNIPAAm Nanoconjugates. Cationized bovine serum albumin (BSA-NH_2) was synthesized by carbodiimide-activated conjugation of 1,6-diaminohexane to aspartic and glutamic acid residues on the external surface of the protein. For this, a solution of 1,6-diaminohexane (1.5 g, 12.9 mmol) was adjusted to pH 6.5 using 5 M HCl and added dropwise to a stirred solution of the protein (200 mg, 2.98 μmol). The coupling reaction was initiated by adding *N*-ethyl-*N*′-(3-(dimethylamino)propyl) carbodiimide hydrochloride (EDAC, 100 mg) immediately and again (50 mg) after 5 h. The pH value was maintained at 6.5 using dilute HCl, and the solution was stirred for a further 6 h. The solution was then centrifuged to remove any precipitate, and the supernatant dialyzed (dialysis tubing 12−14 kDa MWCO) extensively against Milli-Q water.

End-capped mercaptothiazoline-activated PNIPAAm (M_n = 8800 g mol^{-1}, 10 mg in 5 mL of water) was synthesized according to our previous reported method[37] and added to a stirred solution of BSA-NH_2 (10 mg in 5 mL of PBS buffer at pH 8.0). The mixed solution was stirred for 12 h and then purified by using a centrifugal filter (MWCO 50 kDa) to remove any unreacted PNIPAAm and salts. After freeze-drying, the BSA-NH_2/PNIPAAm conjugate was obtained. Based on MALDI-TOF UV−vis spectroscopy measurements, there were 3.3 PNIPAAm chains per BSA molecule.

Membrane Cross-Linking of BSA-NH_2/PNIPAAm Proteinosomes for DNA Encapsulation and Release. DNA (salmon testes, Sigma, bp ∼ 2000, M_w ∼1300 kDa; stained by SYBR green I, Invitrogen (used as received, x10,000 concentrate in DMSO, 1000 times diluted in water) was encapsulated into the proteinosome interior by adding aqueous DNA (20 μL, 2.0 mg/mL) to 40 μL of an aqueous solution of BSA-NH_2/PNIPAAm (4.0 mg/mL) nanoconjugates, followed by addition of 1.0 mL of 2-ethyl-1-hexanol. The proteinosomes were then cross-linked in the continuous oil phase by reaction of free primary amines on the protein surface with bis-*N*-succinimidyl-(nonaethylene glycol) ester (NHS-PEG9 ester; M_w = 709) or a longer chain derivative containing a central disulfide bridge (4,7,10,13,16,19,22,25,32,35,38,41,44,47,50,53-hexadecaoxa-28,29-dithiahexapentacontanedioic acid di-*N*-succinimidyl ester; NHS-PEG16-DS disulfide ester, M_w 1000, Sigma), or mixtures of both cross-linking agents at NHS-PEG16-DS: NHS-PEG9 molar ratios of 1:7, 4:5.6 or 10:2.8. The cross-linked proteinosomes were then transferred into water as follows. After 3 h sedimentation, the upper clear oil layer was discarded, and 0.5 mL of 65% ethanol added and the emulsion gently shaken. The dispersion was then dialyzed against 65% ethanol/water

mixture and then against milli-Q water to complete the phase transfer process. The samples were centrifuged to remove any free DNA in solution produced by fracture of the proteinosomes during transfer into water.

Release of DNA from the proteinosomes was induced by enzyme-mediated disassembly of the NHS-PEG9 ester cross-linked protein–polymer membrane in water. An aqueous dispersion of the DNA-containing proteinosomes was mixed with 20 mL of a buffered protease solution (*Streptomyces griseus*, Sigma, ≥3.5 units/mg solid, M_w ~ 50 kDa; pH 7.4 buffer) at enzyme concentrations of 0.01, 0.005, or 0.0025 mg/mL. Aliquots (2 mL) of the suspension were removed at various time intervals and filtered to remove any intact proteinosomes, and the concentration of released SYBR green I-stained DNA in the bulk phase determined by measuring changes in fluorescence intensity at 522 nm (excitation/emission, 497 nm/522 nm). This procedure was also used to determine the release of encapsulated fluorescently labeled DNA via reductive cleavage of proteinosomes cross-linked with NHS-PEG16-DS disulfide ester or mixtures of NHS-PEG16-DS disulfide ester and NHS-PEG9 ester bridges. In each case, disassembly of the membrane was initiated by addition of glutathione (5 mM) or tris(2-carboxyethyl)phosphine (TCEP) to the proteinosome dispersion.

Hydrogel Assembly and Enzyme Reactivity in Alkaline Phosphatase-Containing BSA-NH_2/PNIPAAm Proteinosomes. Alkaline phosphatase (ALP)-containing proteinosomes were prepared by adding 20 μL of aqueous ALP (1 U/μL) to 40 μL of an aqueous solution of BSA-NH_2/PNIPAAm nanoconjugates (4.0 mg/mL, pH 8.5, 50 mM sodium carbonate buffer), followed by addition of 1.0 mL of 2-ethyl-1-hexanol, and shaking the mixture by hand for 10 s. Under these conditions, and given an average diameter of 20 μm, we estimated the number of droplets to be of the order of 15 million. The proteinosomes were then cross-linked in the continuous oil phase by addition of bis-*N*-succinimidyl-(nonaethylene oxide) ester (0.5 mg, NHS-PEG9 ester; M_w = 709), which reacted with free primary amine groups on the protein surface. Transfer of the cross-linked proteinosomes into water was achieved as described above. The transferred samples were centrifuged to remove any free ALP in solution produced by fracture of the proteinosomes during transfer into water.

Hydrogel formation within the proteinosomes was undertaken by gently mixing 10 μL of an aqueous dispersion of NHS-PEG9 ester cross-linked ALP-containing proteinosomes with or without the addition of 2 μL of Hoechst 33258 dye (1.0 mM) and an aqueous solution of *N*- fluorenylmethylcarbonyl-tyrosine-(*O*)-phosphate (Fmoc-TyrP, Nova-biochem; 2 μmol, 30 μL, alkaline buffer (pH 9.2, 50 mM disodium hydrogen phosphate, 50 mM sodium carbonate, 1 mM magnesium chloride) at a final Fmoc-TyrP concentration of 50 mM. (Control experiments in bulk solution indicated that hydrogelation occurred at Fmoc-TyrP concentrations above 10 mM.) Formation of the fluorenylmethylcarbonyl-tyrosine (Fmoc-TyrOH) hydrogel (typically comprising 2.5 wt % Fmoc-TyrOH) within the proteinosome was investigated by measuring the time-dependent increase in blue fluorescence associated with binding of Hoechst 33258 dye (1.0 mM) to the growing amino acid nanofilaments. In most cases, gelation within the proteinosomes was completed within 7 h. All optical and fluorescence microscopy images were recorded in water in sealed sample holders to prevent dehydration of the proteinosome dispersions over extended time periods.

Studies of enzyme activity of the ALP-encapsulated hydrogel proteinosomes with respect to an auxiliary small molecule substrate were undertaken below and above the gel–sol transition temperature (30 and 45 °C, respectively). Typically, 100 μL of 0.025 M *p*-nitrophenyl phosphate (substrate) and 300 μL of buffer solution (100 mM Tris, pH 8.8, 1 mM $MgCl_2$) was added to the continuous water phase of a 100 μL dispersion of proteinosomes containing encapsulated ALP at a constant temperature. The reaction was monitored by UV–vis spectroscopy at 400 nm for 300 s, and the catalytic reaction rate determined using the extinction coefficient of the product *p*-nitrophenolate (17500 $M^{-1}cm^{-1}$ at pH 8.8 in Tris buffer).

DNA Encapsulation and Release from Membrane-Cross-Linked, Hydrogel-Containing BSA-NH_2/PNIPAAm Proteinosomes. DNA-containing, ALP-loaded proteinosomes were prepared by adding aqueous DNA (20 μL, 0.5 mg/mL; salmon testes, Sigma, bp ~ 2000, M_w ~1300 kDa; tagged with SYBR green I (Invitrogen)) and 20 μL of aqueous ALP (1 U/μL) to 20 μL of an aqueous solution of BSA-NH_2/PNIPAAm (8.0 mg/mL) nanoconjugates, followed by addition of 1.0 mL of 2-ethyl-1-hexanol. The proteinosomes were then cross-linked in the continuous oil phase by reaction of free primary amines on the protein surface with a central disulfide bridge (NHS-PEG16-DS disulfide ester). The cross-linked DNA-ALP-containing proteinosomes were then transferred into water as described before. The samples were centrifuged to remove any free ALP or DNA in solution produced by fracture of the proteinosomes during transfer into water.

Hydrogel formation within the DNA-ALP-containing proteinosomes was undertaken by gently mixing 40 μL of an aqueous dispersion of NHS-PEG16-DS disulfide ester cross-linked DNA/ALP-containing proteinosomes with 5 μL of Hoechst 33258 dye (1.0 mM) and an aqueous solution of *N*- fluorenylmethylcarbonyl-tyrosine-(*O*)-phosphate (Fmoc-TyrP, Nova-biochem; 8 μmol, 120 μL, alkaline buffer (pH 9.2, 50 mM disodium hydrogen phosphate, 50 mM sodium carbonate, 1 mM magnesium chloride) at a final Fmoc-TyrP concentration of 50 mM. Gelation within the proteinosomes was stopped after 7 h by centrifugation (4000 rpm, 4 min) to remove unreacted Fmoc-TryP.

Release of DNA from the hydrogel-modified proteinosomes was induced by protease-, TCEP-, or GSH-mediated disassembly of the cross-linked protein–polymer membrane in water. For this, an aqueous dispersion of the DNA-containing, hydrogel-filled proteinosomes was mixed with 20 mL of a buffered tris(2-carboxyethyl)-phosphine (TCEP) (5.0 mM), glutathione (GSH) (5.0 mM), or protease (50 μg/mL) solution. Aliquots (2 mL) of the suspension were removed at various time intervals and filtered to remove any intact proteinosomes, and the concentration of released SYBR green I-stained DNA in the bulk phase determined by measuring changes in fluorescence intensity at 522 nm (excitation/emission, 497 nm/522 nm).

Fluorescence Labeling of Proteins. Fluorescein isothiocyanate (FITC)-labeled cationized BSA (FITC-BSA-NH_2) was prepared by dissolving a dried powder of the positively charged protein (5.0 mg) in 2.0 mL of pH 8.5 sodium carbonate buffer solution (100 mM), followed by dropwise addition of 50 μL DMSO solution of FITC (1.0 mg/mL). The solution was stirred at room temperature for 5 h, purified by dialyzing against Milli-Q water, and freeze-dried. Rhodamine B isothiocyanate (RBITC)-labeled ALP was prepared by the same procedure using a DMSO solution of RBITC (1.0 mg/mL). The FITC-BSA-NH_2 protein was reacted with end-capped mercaptothiazoline-activated PNIPAAm (see above) to produce fluorescein labeled BSA-NH_2/PNIPAAm nanoconjugates that were used as building blocks for proteinosome assembly.

Acrylic Acid-Modified BSA. Five mL of acrylic acid solution (50 mg, 0.69 mmol) was adjusted to pH 6.5 using 1 mM NaOH and added dropwise to a stirred aqueous solution of cationized BSA (BSA-NH_2, 20 mg, 10 mL, pH 6.5). The reaction was initiated by adding *N*-ethyl-*N*′-(3-(dimethylamino)propyl) carbodiimide hydrochloride (EDAC, 20 mg) immediately, and again (10 mg) after 5 h. The pH value was maintained at 6.5 using dilute HCl, and the solution was stirred for a further 6 h. The solution was then filtered and the supernatant dialyzed (dialysis tubing 12–14 kDa MWCO) extensively against Milli-Q water. The resulting acrylic acid modified protein (BSA-NH_2-AA) was characterized by matrix-assisted laser desorption/ionization time-of-flight mass spectrometry (MALDI-TOF MS). The construct consisted of ca. 17 acrylate groups per molecule. A fluorescently labeled form of BSA-NH_2-AA was prepared by reaction with RBITC using methods described above.

Characterization Methods. Optical and fluorescence microscopies were performed on a Leica DMI3000 B manual inverted fluorescence microscope at 10×, 20×, 40×, and 100× magnification. A fluorescence filter with excitation at 340–380 nm and an emission cut

dx.doi.org/10.1021/ja504213m | *J. Am. Chem. Soc.* 2014, 136, 9225–9234

off at 400 nm was used. Confocal images were obtained on a Leica SP5-II confocal laser scanning microscope attached to a Leica DMI 6000 inverted epifluorescence microscope, equipped with 150 mW Ar laser (458, 476, 488, 514 nm lines), 5 mW solid state green laser (543 nm), and 20 mW red He/Ne (633 nm) diode laser. The 3D images were processed using Volocity 6.0 software (PerkinElmer, USA).

Transmission electron microscopy (TEM) analysis was undertaken on a Jeol 1200 Mk2 TEM using a LaB_6 filament at 120 kV in bright-field mode. Samples were prepared by adding one drop of proteinosome solution (0.1 mg/mL) onto a 300 mesh, carbon film-coated copper grid, and the specimens were then dried in vacuum for 1 day. MALDI-TOF MS was performed on a 4700 Proteomics analyzer (Applied Biosystems) using 2,5-dihydroxybenzoic acid as matrix substance. The sample aqueous solution concentration was 1.0 mg/mL. A Jasco FP-6500 fluorimeter was used for SYBR green I-stained DNA release measurements with an excitation band at 497 nm and excitation and emission band-widths of 3 nm. Fluorescence line intensity profiles were recorded across single proteinosomes and analyzed using Gwyddion software

■ ASSOCIATED CONTENT

Supporting Information

MALDI-TOF MS and UV−vis spectra, molecular structures, optical and fluorescence microscopy images, reaction schemes, hydrogel growth kinetics, shrinkage, and mechanical deformation, AFM images, DNA release profiles. This material is available free of charge via the Internet at http://pubs.acs.org.

■ AUTHOR INFORMATION

Corresponding Author

s.mann@bristol.ac.uk

Notes

The authors declare no competing financial interest.

■ ACKNOWLEDGMENTS

We thank the ERC Advanced Grant scheme (S.M.) and Marie Curie Fellowship (X.H.) scheme for financial support. We thank Jon Jones and Robert Harniman for help with electron and scanning probe microscopy and Katy Jepson for assistance with confocal microscopy.

■ REFERENCES

(1) Nomura, S.-I. M.; Tsumoto, K.; Hamada, T.; Akiyoshi, K.; Nakatani, Y.; Yoshikawa, K. *ChemBioChem* **2003**, *4*, 1172−1175.
(2) Ishikawa, K.; Sato, K.; Shima, Y.; Urabe, I.; Yomo, T. *FEBS letters* **2004**, *576*, 387−390.
(3) Noireaux, V.; Libchaber, A. *Proc. Natl. Acad. Sci. U.S.A.* **2004**, *101*, 17669−17674.
(4) Walde, P.; Ichikawa, S. *Biomol. Eng.* **2001**, *18*, 143−177.
(5) Pontani, L.-L.; Van der Gucht, J.; Salbreux, G.; Heuvingh, J.; Joanny, J.-F.; Sykes, C. *Biophys. J.* **2009**, *96*, 192−198.
(6) Krishna Kumar, R.; Yu, X.; Patil, A. J.; Li, M.; Mann, S. *Angew. Chem., Int. Ed.* **2011**, *50*, 9343−9347.
(7) Kurihara, K.; Tamura, M.; Shohda, K.-i.; Toyota, T.; Suzuki, K.; Sugawara, T. *Nat. Chem.* **2011**, *3*, 775−781.
(8) Städler, B.; Price, A. D.; Chandrawati, R.; Hosta-Rigau, L.; Zelikin, A. N.; Caruso, F. *Nanoscale* **2009**, *1*, 68−73.
(9) Chandrawati, R.; Hosta-Rigau, L.; Vanderstraaten, D.; Lokuliyana, S. A.; Städler, B.; Albericio, F.; Caruso, F. *ACS Nano* **2010**, *4*, 1351−1361.
(10) Hosta Rigau, L.; Shimoni, O.; Städler, B.; Caruso, F. *Small* **2013**, *9*, 3573−3583.
(11) Wilson, D. A.; Nolte, R. J.; van Hest, J. C. *Nat. Chem.* **2012**, *4*, 268−274.
(12) Marguet, M.; Bonduelle, C.; Lecommandoux, S. *Chem. Soc. Rev.* **2013**, *42*, 512−529.
(13) Peters, R. J.; Louzao, I.; van Hest, J. C. *Chem. Sci.* **2012**, *3*, 335−342.
(14) van Dongen, S. F.; Nallani, M.; Cornelissen, J. J.; Nolte, R. J.; van Hest, J. *Chem.—Eur. J.* **2009**, *15*, 1107−1114.
(15) Li, M.; Green, D. C.; Anderson, J. R.; Binks, B. P.; Mann, S. *Chem. Sci.* **2011**, *2*, 1739−1745.
(16) Li, M.; Harbron, R. L.; Weaver, J. V.; Binks, B. P.; Mann, S. *Nat. Chem.* **2013**, *5*, 529−536.
(17) Krishna Kumar, R.; Li, M.; Olof, S. N.; Patil, A. J.; Mann, S. *Small* **2013**, *9*, 357−362.
(18) Li, M.; Huang, X.; Mann, S. *Small* **2014**, DOI: 10.1002/smll.201400639.
(19) Keating, C. D. *Acc. Chem. Res.* **2012**, *45*, 2114−2124.
(20) Andes-Koback, M.; Keating, C. D. *J. Am. Chem. Soc.* **2011**, *133*, 9545−9555.
(21) Sokolova, E.; Spruijt, E.; Hansen, M. M.; Dubuc, E.; Groen, J.; Chokkalingam, V.; Piruska, A.; Heus, H. A.; Huck, W. T. *Proc. Natl. Acad. Sci. U.S.A.* **2013**, *110*, 11692−11697.
(22) Strulson, C. A.; Molden, R. C.; Keating, C. D.; Bevilacqua, P. C. *Nat. Chem.* **2012**, *4*, 941−946.
(23) Koga, S.; Williams, D. S.; Perriman, A. W.; Mann, S. *Nat. Chem.* **2011**, *3*, 720−724.
(24) Williams, D. S.; Koga, S.; Hak, C. R. C.; Majrekar, A.; Patil, A. J.; Perriman, A. W.; Mann, S. *Soft Matter* **2012**, *8*, 6004−6014.
(25) Crosby, J.; Treadwell, T.; Hammerton, M.; Vasilakis, K.; Crump, M. P.; Williams, D. S.; Mann, S. *Chem. Commun.* **2012**, *48*, 11832−11834.
(26) Tang, T.-Y. D.; Antognozzi, M.; Vicary, J. A.; Perriman, A. W.; Mann, S. *Soft Matter* **2013**, *9*, 7647−7656.
(27) Tang, T.-Y. D.; Hak, C. R. C.; Thompson, A. J.; Kuimova, M. K.; Williams, D. S.; Perriman, A. W.; Mann, S. *Nat. Chem.* **2014**, *6*, 527−533.
(28) Williams, D. S.; Patil, A. J.; Mann, S. *Small* **2014**, *10*, 1830−1840.
(29) Stano, P.; Luisi, P. L. *Curr. Opin. Biotechnol.* **2013**, *24*, 633−638.
(30) Hammer, D. A.; Kamat, N. P. *FEBS letters* **2012**, *586*, 2882−2890.
(31) Goff, L. L.; Lecuit, T. *Science* **2009**, *324*, 1654−1655.
(32) Brangwynne, C. P. *J. Cell Biol.* **2013**, *203*, 875−881.
(33) Budin, I.; Szostak, J. W. *Proc. Natl. Acad. Sci. U.S.A.* **2011**, *108*, 5249−5254.
(34) Mann, S. *Acc. Chem. Res.* **2012**, *45*, 2131−2141.
(35) Mann, S. *Angew. Chem., Int. Ed.* **2013**, *52*, 155−162.
(36) Pohorille, A.; Deamer, D. *Trends Biotechnol.* **2002**, *20*, 123−128.
(37) Huang, X.; Li, M.; Green, D. C.; Williams, D. S.; Patil, A. J.; Mann, S. *Nat. Commun.* **2013**, *4*, 2239 DOI: 10.1038/ncomms3239.
(38) Huang, X.; Li, M.; Mann, S. *Chem. Commun.* **2014**, *50*, 6278−6280.
(39) Vargo, K. B.; Parthasarathy, R.; Hammer, D. A. *Proc. Natl. Acad. Sci. U.S.A.* **2012**, *109*, 11657−11662.